Dr. Robert E. Hebner, John D. Herbst, Angelo L. Gattozzi

Intelligent Microgrid Demonstrator

ABSTRACT

The Center for Electromechanics at the University of Texas at Austin has a microgrid demonstrator capable of operating at power levels up to 2 MW. The microgrid is designed to interface with the commercial power system and other distributed sources of electric power, both ac and dc. It incorporates local prime movers that drive generators, both conventional 60 Hz and high frequency ac (800 Hz), as well as energy storage units. The microgrid is designed as a flexible system, easily expandable in power and re-definable in terms of voltage levels and system configuration.

Several grid architectures have been studied and simulated, including a variety of pulsed and intermittent duty loads, as they can be found on US Navy ships. One problem under investigation is that of dc bus stability under the influence of constant power loads: these loads are known to induce instability at kW power levels but experimental data is very limited at MW power levels which are more representative of the situation on a ship.

This paper describes the microgrid architecture, simulation results and data collected to date, as well as plans to demonstrate critical issues like stability, reconfigurability, fault management, integration of renewables, and model validation.

INTRODUCTION

The power system of an electric ship resembles a smart microgrid, but also has characteristics that make it unique. Like its land based counterpart, the electric ship power system is designed to be autonomous, highly reliable, capable of delivering high quality power to all loads, and organized as a flexible distribution network that can be reconfigured depending on need. Shipboard loads, however, have characteristics and requirements that vary widely, ranging from continuous duty loads, like hotel loads and propulsion loads, to intermittent duty loads, such as directed energy weapons. For these reasons, the power system of an electric ship is likely to be characterized by the following distinctive features:

1. A close matching of the total power demanded by the loads to the available generating capacity with smaller excess margin
2. Reliance on energy storage to support pulsed loads.

The technical challenges associated with microgrids include the increasing incidence of power electronic conversion stages, the coexistence on the same infrastructure of ac-based networks and dc-based sections, the presence of generating units relying on nontraditional energy resources alongside traditional generators, and the gradual migration from a highly centralized control architecture to one relying more on local intelligence and decisional autonomy. Because of the obvious complexities and varieties of microgrid structures, it is fair to say that, while the theoretical understanding of the issues involved and the computer simulation efforts are being pursued vigorously by the technical community at large, the experimental database needed to support the large scale implementation of smart microgrids is still very limited. Several tests of reduced scale systems have been performed at power levels of a few kW (Kwasinski and Onwuchekwa, to be published; Awan et al., 2009; Kwasinski and Krein, 2007), some at few hundred kW (California Electric Reliability Technology Solutions 2009-2010), but little has been done at MW power levels. If this is true for land-based systems, it is even more so for shipboard power systems in view of the variety of load characteristics mentioned above.

To move forward in this crucial area of generating data needed for the design of effective, efficient, and reliable power systems for electric ships, the Center for Electromechanics at the University of Texas at

Austin (CEM-UT) established a microgrid demonstrator capable of operating initially at power levels up to 2 MW, but expandable in power and re-definable in terms of voltage levels and system configuration. This paper describes the plans for this microgrid and some of the preliminary work performed.

MICROGRID ARCHITECTURE

The first stage of development of the CEM-UT microgrid is rated at 2 MW of power with a foreseeable expansion to 10 MW during a second phase. Although considerable, these power levels would still be small (less than 10%) when compared to the total power capacity of a ship. Thus, the microgrid is planned to be interfaced with the commercial power system so that, while it is designed to represent a particular section of a ship's system, it is also connected to a live power network corresponding to the rest of the system, as it would be in an actual ship.

The microgrid comprises a number of distributed local prime movers driving generators and other power supplies:

1. Two diesel-powered 60 Hz generators rated at 1 MW each
2. One turbine-driven 800 Hz generator rated at 1.5 MW
3. One variable voltage dc supply derived from the 60 Hz utility or a separate diesel powered generator rated at 300 kW
4. Renewable energy sources to be inserted in a future expansion
5. DC storage units (batteries, capacitors) also to be added in a future expansion

Of particular interest is an energy storage system consisting of a composite flywheel riding on magnetic bearings and capable of storing 480 MJ of energy, interfaced to the rest of the system via a 2 MW induction machine and a bidirectional power converter.

These supplies are interconnected, after proper voltage transformation stages, using a common dc bus. Initially the bus is scheduled to operate at 1,100 Vdc, moving up to 1,960 Vdc in the second development phase. The common dc bus architecture has been chosen as this seems to be a good candidate for grid interconnection both for shipboard and land-based systems.

The dc bus is connected to a variety of loads, either directly or via converters, that can provide power to common 60 Hz type loads. In a future expansion, the dc bus will also be interfaced with the commercial power grid. A one line circuit diagram showing the microgrid as it is being assembled for phase one is shown in Figure 1. In Figures 2-4, a general view of the physical area covered by the microgrid is also shown, together with some of the equipment being assembled per the system of Figure 1.

The microgrid components are divided between two main locations interconnected by the dc bus: the first location is in a laboratory in the main building and the second is in a separate building with reinforced walls suitable for safely operating devices with high kinetic energy, like turbines, flywheel, and high-speed machines. The dc bus between these two locations is in an underground trench (Figures 2 and 3). A summary of pertinent data on the dc bus is given in Table 1.

Table 1. Data of CEM-UT DC Bus

Bus length	31 m
Conductor size	AWG535 DLO cable
Number of conductors	2 parallel
Series Resistance	0.13 mΩ/m
Series Inductance	0.32 μH/m
Shunt Capacitance	0.04 nF/m

Many components comprising the microgrid have been developed over time and tested individually or as part of larger systems. In fact, the University researcher team has had the opportunity to consider various topologies of microgrids and to investigate their performance. This has led, for example, to the development of large computer simulations to study the behavior of a ship's electrical system under different operational scenarios (Ouroua et al., 2009; Herbst and Gattozzi, 2008.). These preceding studies have provided invaluable insights in the understanding of both the physical behavior of microgrid components and the capabilities and limitations of commercially available simulation programs.

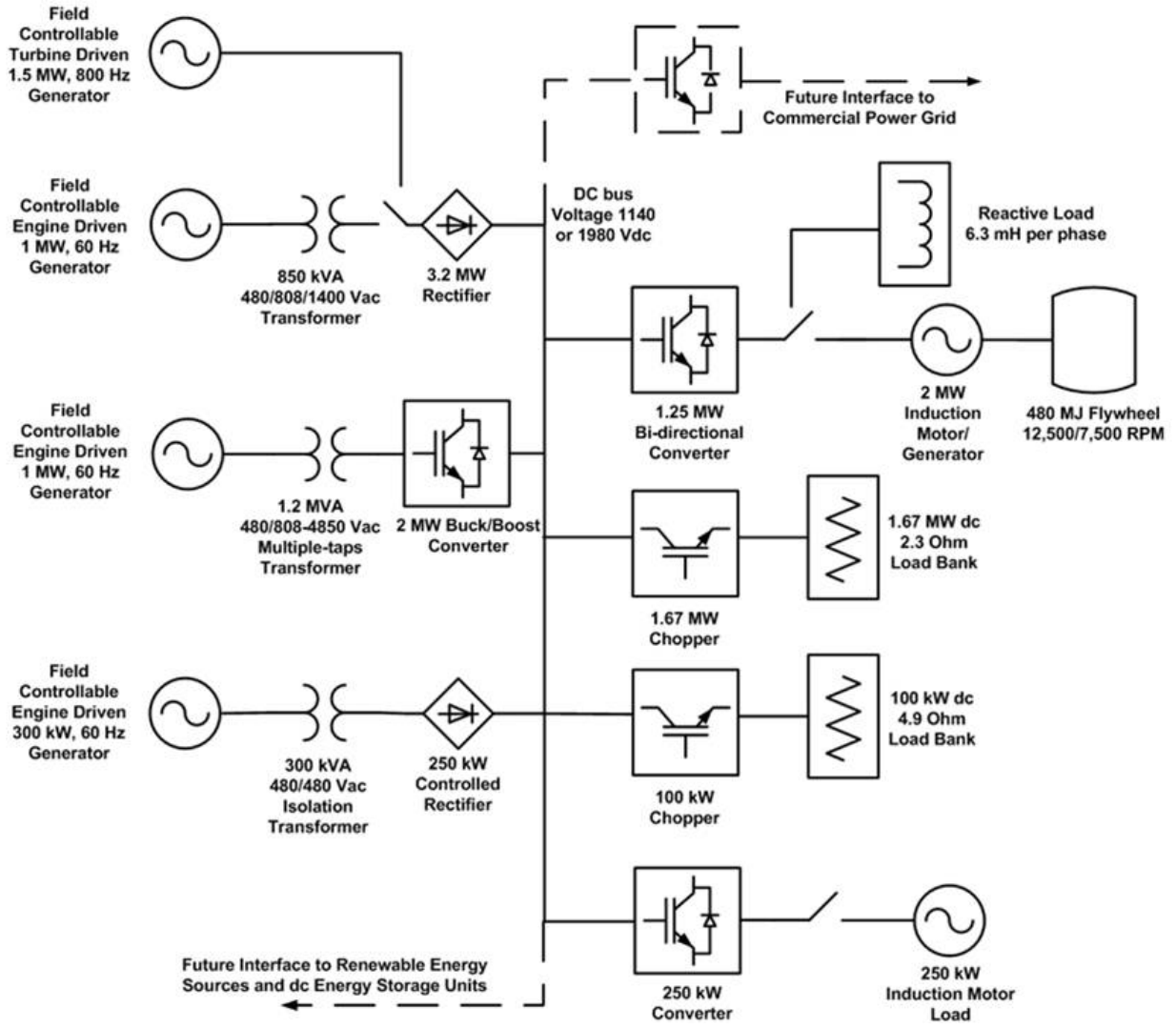

Figure 1. Schematic Diagram of Phase One of the CEM-UT Microgrid (Circuit Protection and Auxiliary Units Not Shown)

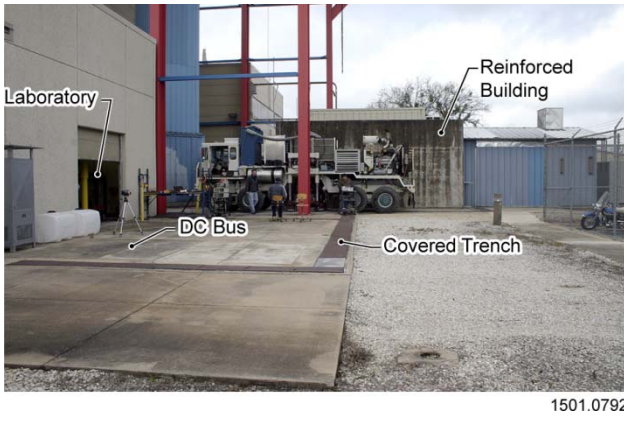

Figure 2. View of the Reinforced Building, Laboratories (left), and Connecting DC Bus (underground metal covered trench)

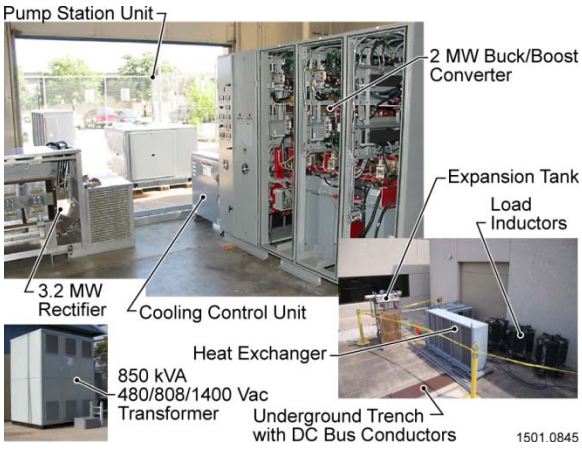

Figure 3. View from Inside Lab (top), Outside Lab (right), and Outside Bunker (lower left)

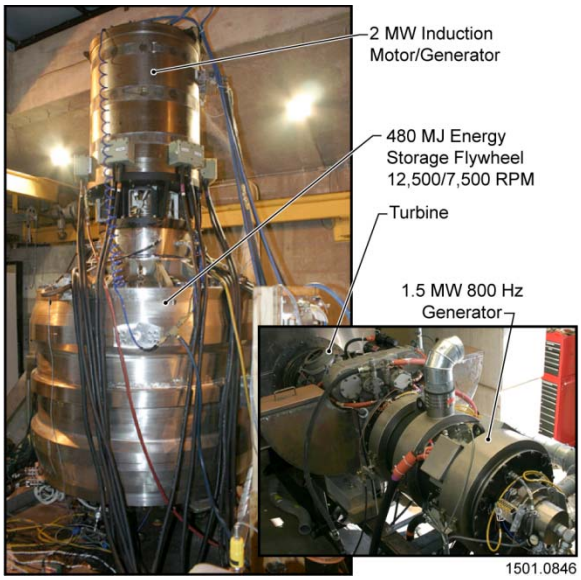

Figure 4. Partial Views of the Inside of the Bunker Showing the Flywheel Energy Storage System and the High Speed Generator

PRELIMINARY INVESTIGATIONS

As the microgrid is being assembled and tested, some preliminary investigations have been initiated. As a required first step, comprehensive models of the microgrid are being developed. These models will allow high fidelity representations of the components of the microgrid and the detailed study of their interactions under various operational conditions.

Some preliminary studies and tests are being conducted on subassemblies. One of the key issues with a microgrid based on a common dc bus topology is the stability of the dc bus under transient conditions occurring both on the supply side and the load side. These events have been studied in some detail by means of computer simulations of a common dc bus (Figure 5). Here the dc bus is supported by one turbo-generator and two flywheel energy storage units. Simulations under different conditions have shown that the system can be stable if the output of the flywheel generators is controlled by means of active rectifiers. Two typical simulation results under transient conditions are reported in Figures 6 and 7 (Herbst and Gattozzi, 2008).

The loads that were used in the simulations leading to these results were conventional loads (resistive, motoring loads, etc.). The dc bus loading by the electronic power converters shown in Figure 5 was also, in a sense, conventional, as the load power was not controlled very tightly. A different case is presented by loads of the constant power type. These loads are the result of the recent advances in power electronics that make possible the tight regulation of converter outputs over a very narrow band (e.g., the power supplies of many types of electronic equipment, like computers, or electromechanical systems with precise control of speed and position).

It is well known that constant power loads can be sources of instabilities for the dc bus at least in kW class installations (Belkhayat, Cooley, and Witulski, 1995; Gadoura et al., 1998). Consequently, it is important to assess if these types of loads may also induce instabilities, with potentially deleterious results, in MW class systems.

The literature on power system instabilities driven by constant power loads has been steadily growing in the last four decades and several methods have been used to analyze the phenomenon (Sudhoff et al., 2002; Andrus, Edrington, and Steurer, 2009). The issue of constant power loads can be summarized as follows: assuming that a load truly demands constant power from a dc bus, if for some external perturbation the dc bus were to sag temporarily, such load would react to the lowering of the system voltage by drawing a larger amount of current. This current surge would tend to further reduce the system voltage leading eventually to an oscillation, if not a complete collapse, of the bus.

Analytically, if P is the power demanded by the load, v is the bus voltage at the load, and i_P is the current drawn by the load, then the condition of an ideal constant power load is expressed by

$$P = const = vi_P \qquad (1)$$

from which we derive

$$i_P = \frac{P}{v} \qquad (2)$$

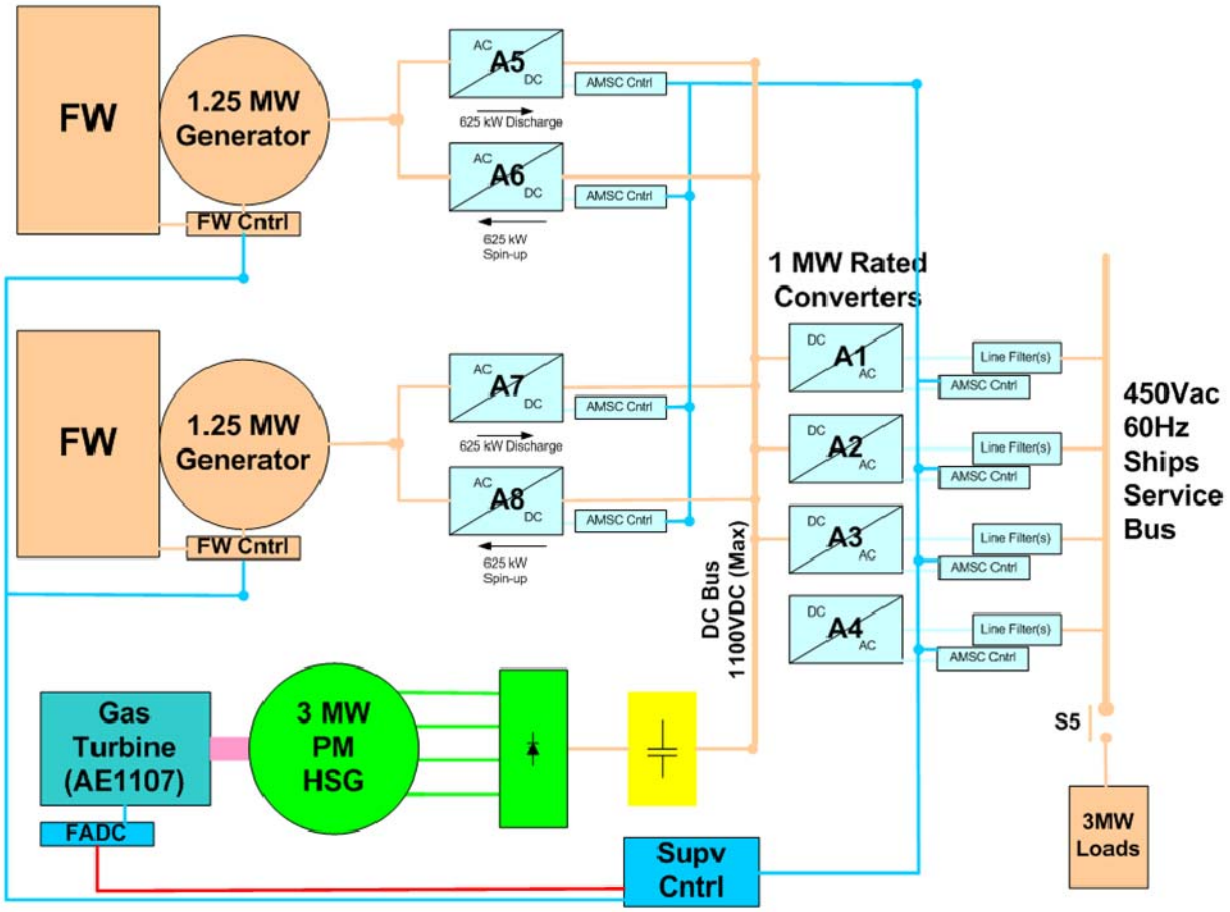

Figure 5. Conceptual Microgrid with Common DC Bus, Local Generation, and Energy Storage for a System Intended to Provide Auxiliary Power to the Main AC Bus of a U.S. Ship

The problem of requiring an infinite current at zero voltage implied by (2) will be shown later to be of no concern in a real system, so that we can use the idealized expression (2) without recurring to complicated notations. The change in current in response to a change in voltage is, from (2)

$$\frac{di_P}{dv} = -\frac{P}{v^2} \tag{3}$$

and we can now define ρ as the differential resistance presented by the load to the dc bus

$$\rho = \frac{dv}{di_P} = -\frac{v^2}{P} < 0 \tag{4}$$

Note that the total input resistance of the load, R_{load}, remains positive,

$$R_{load} = \frac{v}{i_P} = \frac{v^2}{P} > 0 \tag{5}$$

but its differential resistance, namely the resistance to changes on the dc bus, is indeed negative. This is the root of potential instabilities.

If we consider the simplified equivalent circuit in Figure 8 to represent a dc bus of voltage v and capacitance C, supplied by a dc source E of internal impedance R_s via the line inductance L and line resistance R, and with the bus itself connected to a constant power load drawing a power $P = const$ and to additional conventional loads represented by the equivalent resistance R_e, we can write equations

$$\begin{aligned} E &= L\frac{di}{dt} + (R_s + R)i + v \\ i &= C\frac{dv}{dt} + \frac{v}{R_e} + \frac{P}{v} \end{aligned} \tag{6}$$

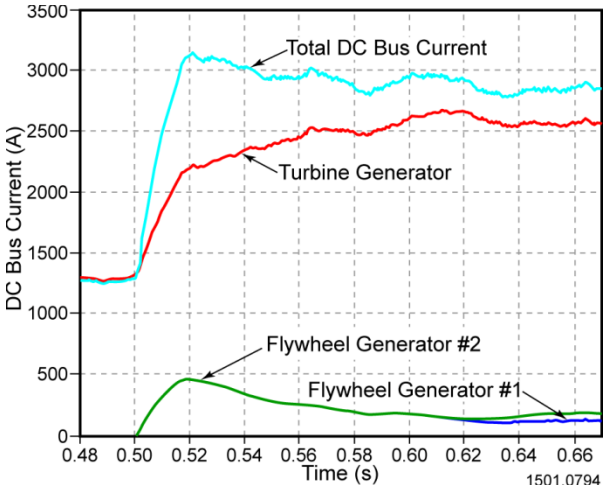

Figure 6. In the system of Figure 5, the load is stepped from 1 MW to 2 MW at *t* = 0.5 s. The currents into the dc bus from the turbine and the two flywheel generators, and the total current, are shown (load leveling)

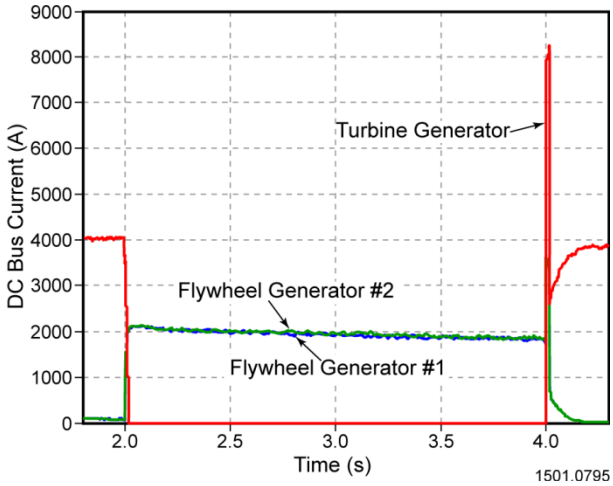

Figure 7. The turbine goes off-line at *t* = 2 s and the load is carried by the two flywheel generators. At *t* = 4 s the turbine generator is reconnected and, after an initial current spike, it picks up the load again (UPS function)

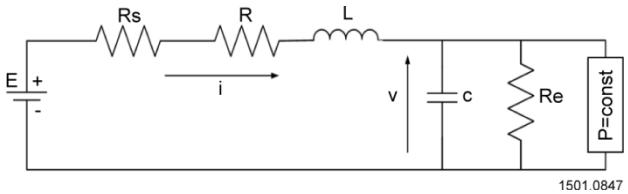

Figure 8. Simple Model of a Constant Power Load Fed by a DC Bus

which yield the single equation for v

$$LC\frac{d^2v}{dt^2}+\frac{L}{R_e}+\left(R_1C-\frac{LP}{v^2}\right)\frac{dv}{dt}+\left(1+\frac{R_1}{R_e}\right)v=E-\frac{R_1P}{v} \tag{7}$$

where we have set

$$R_1=R_S+R \tag{8}$$

Equation (7) is non-linear and its general solution does not appear to be known. Earlier work sought approximate solutions in a variety of ways, not always easy to reconcile with each other. Here we shall offer some general considerations that, though far from solving explicitly equation (7), attempt to attain a global view and possibly some general insights into the problem. For ease of notation we shall adopt the following definitions:

$$\begin{aligned}\omega_o&=\frac{1}{\sqrt{LC}}\\ \tau_C&=R_eC\\ \tau_L&=\frac{L}{R_1}\\ \frac{1}{\tau}&=\frac{1}{\tau_C}+\frac{1}{\tau_L}\\ \omega_1&=\omega_o\sqrt{1+\frac{R_1}{R_e}}\end{aligned} \tag{9}$$

Then equation (7) can be written as

$$\frac{d^2v}{dt^2}+\left(\frac{1}{\tau}-\frac{P}{Cv^2}\right)\frac{dv}{dt}+\omega_1^2v=\omega_o^2v\left(E-\frac{R_1P}{v}\right) \tag{10}$$

and letting

$$\zeta\left[v(t)\right]=\frac{1}{2}\left(\frac{1}{\tau}-\frac{P}{Cv^2}\right) \tag{11}$$

$$f\left[v(t)\right]=\omega_o^2\left(E-\frac{R_1P}{v}\right) \tag{12}$$

$$\omega=\sqrt{\zeta^2-\omega_1^2} \tag{13}$$

we have

$$\frac{d^2v}{dt^2} + 2\zeta\frac{dv}{dt} + \omega_1^2 v = f \qquad (14)$$

which is recognized as the equation of a forced oscillator with frequency ω, decay factor ζ, and forcing function f. The complication arises from the fact that ζ, f, and ω are nonlinear functions of v given by (11), (12), and (13). Some semi-quantitative deductions can nevertheless be made by making a parallel with the equation of the oscillator with constant coefficients.

If this were the case of the simple oscillator with constant decay factor, we know that the solution would be given by a function of the type

$$v = Ve^{-\zeta t}\sin\left(\omega t + \varphi\right) + w(t) \qquad (15)$$

for example, for the case when ω in (13) is imaginary, with V and φ being constants dependent on the initial conditions and $w(t)$ being a particular solution dependent on f.

If we make a formal analogy between this elementary case and the non-linear one, we can see that the origin of the instability lies in the possibility of ζ being negative, which would cause an unbounded response in time. This happens when

$$\zeta < 0 \;\rightarrow\; \frac{Cv^2}{\tau} < P \qquad (16)$$

This condition matches the one reported in (Kwasinski and Onwuchekwa, 2009), where the result was derived for the case of a dc-dc buck converter feeding a constant power load.

Furthermore, from (10), we can say that if there are any stable steady states, they will be given by the solution of the following algebraic equation for v:

$$\omega^2 v = \omega_o^2\left(E - \frac{R_1 P}{v}\right) \qquad (17)$$

with solutions given by

$$v = \frac{E_1}{2} \pm \sqrt{\left(\frac{E_1}{2}\right)^2 - R_P P} \qquad (18)$$

where

$$E_1 = \frac{R_e}{R_e + R_1}E \qquad (19)$$

and

$$R_P = \frac{R_e R_1}{R_e + R_1} \qquad (20)$$

are recognized respectively, as the steady state value of the output voltage v in the absence of the constant power load after all transients have died down, and the parallel combination of R_e and R_1. Thus, quantities in (19) and (20) also coincide with the values of the dc Thevenin equivalent of the circuit as seen by the constant power load.

It will also be noted from (11) and (15) that, in the case of instability, while the voltage will tend to rise exponentially because of a negative value of decay factor, at the same time the decay factor will tend to become less negative as the voltage increases, and concomitantly, from (12), the forcing function becomes less nonlinear approaching more and more the one provided by the constant input supply voltage. When the voltage is large enough that (16) is violated, the decay factor becomes positive again. We can expect, therefore, that an interval of voltage growth, initiated by a negative decay factor, will be followed by one of decaying voltage due to the decay factor becoming positive, and so on. The result, therefore, will be an oscillatory behavior of the voltage in time around one of the values given in (18). It is in light of this that we could ignore, as mentioned previously, to a first approximation the case of voltages close to zero, leading to infinite current, since as the voltage decreases, the decay factor becomes more and more negative, forcing the greater growth of the voltage.

Regarding the solutions (18), they are real if the following relationship is satisfied

$$R_P \le \frac{E_1^2}{2P} \qquad (21)$$

It can be noted that (18) and (21) have a geometrical interpretation: steady state equilibrium solutions exist only if the load curves representing the supply and the load have common points. Thus, if the circuit of Figure 8

is properly recast in its dc Thevenin equivalent mentioned above as shown in Figure 9, the load curve of the power supply is given by

$$E_1 - i_P R_P = v \qquad (22)$$

while the load curve of the constant power load is given by (2). Both these curves are sketched also in Figure 9, which gives a visual interpretation of condition (21). These results are the same as those of Belkhayat, Cooley, and Witulski, (1995). Our analysis, however, does not lead also to a minimum for the value of R_p, which is another result reported in Belkhayat, Cooley, and Witulski, (1995) on the basis of a mixed potential method. It would seem that requiring a minimum value for this resistance would necessarily lead to a minimum source resistance, which is difficult to interpret and that intuitively would lead to unacceptable losses.

It should also be noticed that, while the voltage oscillates, the forcing function also varies and may even change sign as implied by (12). This, of course, further complicates the system's response.

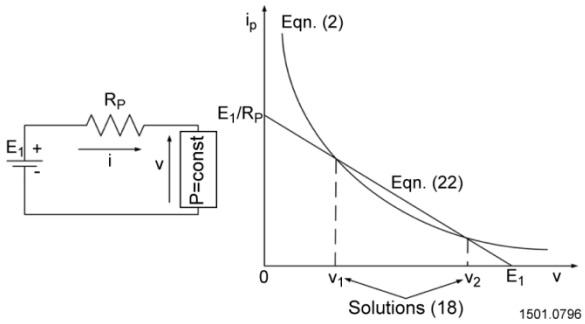

Figure 9. DC Thevenin Equivalent of Circuit in Figure 8 and Graphical Solutions Based on Load Curves

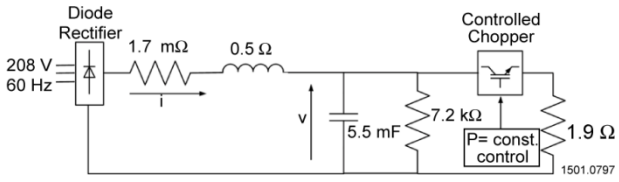

Figure 10. Experimental Circuit Used to Verify Formulas Derived

To assess the sensitivity of the microgrid to potential instabilities and validate some of the predictions summarized above, tests have been initiated on some subassemblies. Specifically, a circuit similar to that of Figure 8 was assembled and tested. The source was implemented with a simple passive rectifier fed from the commercial power lines, and this same source was in turn the power supply for a controlled chopper loaded by a resistor (see Figure 10).

The chopper was controlled in such a way as to keep the power into the load resistor constant, emulating a constant power load. The circuit components are listed in Table 2.

Table 2: Circuit Components

Input ac power	208/480 V, 0 Hz
Output dc bus voltage from the passive diode rectifier	280/650 V dc
Line inductor	0.5 mH
Line resistance	1.7 mΩ
Bus capacitance	5.5 mF
Load resistance (controlled as a constant power load P)	1.9 Ω
Case 1: Constant power load P	15 kW
Case 1: Output voltage v	235 V dc
Case 2: Constant power load P	21.5 kW
Case 2: Output voltage v	212 V dc

Based on the theory presented, if we set our control for the two constant power loads in the tests at 15 kW and 21.5 kW respectively we have the results in Table 3 (input power is 208 V, 60 Hz).

Table 3: Expected Results for Two Test Cases

Constant Power Load kW	Stability Criterion per (16)	Existence of Stable states per (21)
15	1,033 < 15,000 unstable	23,058,824 > 15,000 ok
21.5	840 < 21,500 unstable	23,058,824 > 21,500 ok

Therefore, in both cases we would expect a strong likelihood of unstable behavior around some equilibrium dc bus voltage of finite value.

The tests do not confirm this prediction. Typical traces of voltage and current vs. time for the two cases considered are reported in Figures 11 and 12, which do show some variability in the dc bus, but the excursions are not excessive and certainly not greater than those usually observed on rectified power busses in actual operation.

The explanation of this inconsistency between theory and experimental data results from the experiment being different from the theoretical assumptions, which is a key justification for validation testing. Specifically, the definition of constant power load in (1) and (2) intrinsically assumed an instantaneous response of the system to any voltage changes; the current is immediately adjusted to any change in voltage in order to keep the power constant. This is not realizable in practice, particularly in large scale systems. Any control loop adjusting the current will act in a finite non-zero time. In our case, the controller was sampling voltage points at a 1 kHz rate and calculated a running average of the last 10 voltage points which was then used as the controlling variable for the current output of the controlled rectifier. Thus, not only the sampling rate was slow, but the voltage data were also smoothed.

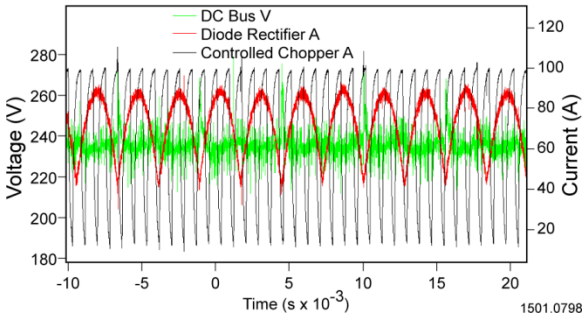

Figure 11. Test of Circuit in Figure 9 with Constant Power Load of 15 kW (208 V, 60 Hz Input)

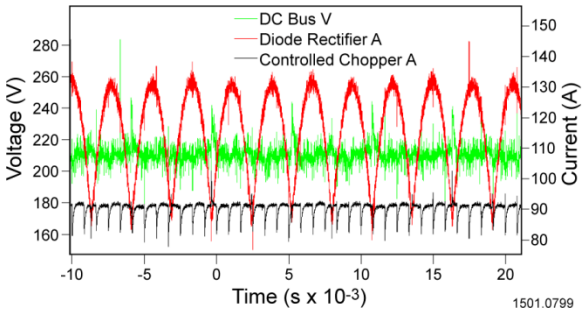

Figure 12. Test of Circuit in Figure 9 with Constant Power Load of 21.5 kW (208 V, 60 Hz Input)

A second phase of testing will use a much faster system. In this way, the microgrid will be used to determine if that controller was the sole component ensuring stability. This is important for model validation.

The results to date support what has been reported, namely that the instabilities caused by constant power loads can be abated by modifying the feedback control loop. Some of the methods proposed include, for example, correcting for the nonlinear elements of equation (7) by using nonlinear feedback (Awan et al., 2009; Emadi et al., 2006), inserting virtual damping resistances (Kwasinski and Krein, 2007), introducing time delays (Aroudi and Orabi, 2010), adding massive capacitance to the dc bus (Tang and Qi, 2009), or in general in some way decreasing the sensitivity of the control system to instantaneous voltage variations.

CONCLUSION

The microgrid at CEM-UT has been described in its phase one architecture and plans for its future extension have been sketched. The microgrid will serve as a test bed to study components and subsystems and their interactions at the MW power level, which is of particular interest to shipboard as well as land installations.

Examples of the simulation efforts undertaken to evaluate the behavior of alternate grid structures have been given. The potential for instabilities introduced by constant power loads on the dc bus has been reviewed and the conditions for the onset of these instabilities have been summarized. The results of tests in this important area have also been given.

The grid assembly and the sectional tests are continuing. The plan is to continue with studies, simulations, and validations tests that would shed light on critical issues like grid stability, reconfigurability, fault management, and the integration of renewables and energy storage.

REFERENCES

Andrus M., C.S. Edrington, and M. Steurer, “Applying multi-terminal dc system control concepts to a multi-zonal, shipboard MVDC power system,” to be published, received Nov. 2009.

Awan, A., B. Nhid-Mobarakeh, S. Pierfederici, and F. Meibody-Tabar, “Nonlinear stabilization of a dc-bus supplying a constant power load,”

IEEE Ind. Appl. Soc. Ann. Mtg., pp. 1-8, Oct. 4-9, 2009.

Belkhayat, M., R. Cooley, and A. Witulski, "Large signal stability criteria for distributed systems with constant power loads," 26th IEEE Power Electron. Spec. Conf., vol. 2, pp. 1333-1338, June 18-22, 1995.

California Electric Reliability Technology Solutions (CERTS): CERTS micro-grid test bed demonstration with American Electric Power, http://certs.lbl.gov/certs-derkey-mgtb.html, accessed December 2009-March 2010.

El Aroudi A. and M. Orabi, "Stabilizing technique for AC-DC boost PFC converter based on time delay feedback," *IEEE Trans. Ckt. & Syst.-II: Expr. Briefs*, vol. 57, no. 1, pp. 56-60, Jan. 2010.

Emadi A., A. Khaligh, C.H. Rivetta, and G.A. Williamson, "Constant power loads and negative impedance instability in automotive systems: definition, modeling, stability, and control of power electronic converters and motor drives," *IEEE Trans. Veh. Techn.*, vol. 55, no. 4, pp. 112-1125, July 2006.

Gadoura I., V. Grigore, J. Hatonen, J. Kyyra, P. Vallittu, and T. Suntio, "Stabilizing a Telecom power supply feeding a constant power load," 20th Int'l Telecomm. Energy Conf., pp. 243-248, Oct. 4-8, 1998.

Herbst, J.D. and A. Gattozzi, ONR Grant N00014-06-0886 "ONR Megawatt Power Module for Ship Service" Final Report, Nov. 16, 2008.

Kwasinski, A. and C.N. Onwuchekwa, "Dynamic behavior of dc micro-grids with instantaneous constant-power loads," to be published, received Nov. 2009.

Kwasinski, A. and P.T. Krein, "Stabilization of constant power loads in dc-dc converters using passivity- based control," 29th Int'l Telecomm. Energy Conf., pp. 867-874, Sept. 30-Oct. 4, 2007.

Ouroua, A., B. Murphy, J. Herbst, and R. Hebner, "Modeling of electric ship power systems," Conf. on Grand Challenges in Model. & Simul. (GCMS'09), pp. 191-197, July 13-16, 2009.

Sudhoff S.D., S.D. Pekarek, S.F. Glover, S.H. Zak, E. Zivi, J.D. Sauer, and D.E. Delisle, "Stability analysis of a dc power electronics based distribution system," SAE 2002.

Tang X. and Z. Qi, "Stability study of DC DPS and the improvement with EDLC," Int'l Conf. Sustain. Power Gen. & Supply, pp. 1-5, Apr. 6-7, 2009.

ACKNOWLEDGMENTS

This work was supported by ONR under Grant no. N00014-08-1-0080.

Dr. Robert E. Hebner, *the principal author, is the Director of the Center for Electromechanics at the University of Texas at Austin. The Center develops advanced energy technology and teams with companies to get the technology to market. Previously, he was acting Director of NIST with an annual budget of about $750 million. He worked in OMB on the technology portions of the Administration's 1990 budget and at DARPA to advance semiconductor manufacturing. He has extensive experience in measurement systems needed to support global trade and in developing government technology programs to stimulate the economy. He is a fellow of the IEEE.*

John D. Herbst *joined the Center for Electromechanics in 1985. He is currently the Principal Investigator for research programs involving high power rotating electric machines and power converters. Prior to his current position, Mr. Herbst served as Principal Investigator for the ONR Megawatt Power Module for Ship Service program, an effort to explore high speed generators and energy storage flywheels to reduce fuel consumption on the DDG51 class of Navy warships. He was also Co-Principal for the Advanced Locomotive Propulsion System (ALPS) project, a $30M effort to demonstrate an advanced hybrid electric propulsion system for high speed passenger locomotives.*

Dr. Angelo L. Gattozzi *joined the Center for Electromechanics at the University of Texas at Austin in 2000. His main focus has been on*

power modules for the electric gun program, resonant converters for high speed motors/generators with flywheel energy storage, design of special generators for energy harvesting from sea waves, and modeling the electric system with energy storage of the DDG51 class Navy destroyer and of some Army Tactical Operating Centers including renewable energy resources.